OPEN

Citation: Transl Psychiatry (2014) 4, e418; doi:10.1038/tp.2014.64

www.nature.com/tp

ORIGINAL ARTICLE

Association of aberrant neural synchrony and altered GAD67 expression following exposure to maternal immune activation, a risk factor for schizophrenia

DD Dickerson[1,2,4], KA Overeem[1,2,3,4], AR Wolff[1,2], JM Williams[2,3], WC Abraham[1,2] and DK Bilkey[1,2]

A failure of integrative processes within the brain, mediated via altered GABAergic inhibition, may underlie several features of schizophrenia. The present study examined, therefore, whether maternal immune activation (MIA), a risk factor for schizophrenia, altered inhibitory markers in the hippocampus and medial prefrontal cortex (mPFC), while also altering electroencephalogram (EEG) coherence between these regions. Pregnant rats were treated with saline or polyinosinic:polycytidylic acid mid-gestation. EEG depth recordings were made from the dorsal and ventral hippocampus and mPFC of male adult offspring. Glutamic decarboxylase (GAD67) levels were separately assayed in these regions using western blot. GAD67 expression was also assessed within parvalbumin-positive cells in the dorsal and ventral hippocampus using immunofluorescence alongside stereological analysis of parvalbumin-positive cell numbers. EEG coherence was reduced between the dorsal hippocampus and mPFC, but not the ventral hippocampus and mPFC, in MIA animals. Western blot and immunofluorescence analyses revealed that GAD67 expression within parvalbumin-positive cells was also reduced in the dorsal hippocampus relative to ventral hippocampus in MIA animals when compared with controls. This reduction was observed in the absence of parvalbumin-positive neuronal loss. Overall, MIA produced a selective reduction in EEG coherence between the dorsal hippocampus and mPFC that was paralleled by a similarly specific reduction in GAD67 within parvalbumin-positive cells of the dorsal hippocampus. These results suggest a link between altered inhibitory mechanisms and synchrony and, therefore point to potential mechanisms via which a disruption in neurodevelopmental processes might lead to pathophysiology associated with schizophrenia.

Translational Psychiatry (2014) **4,** e418; doi:10.1038/tp.2014.64; published online 29 July 2014

INTRODUCTION

Schizophrenia is an illness characterized by a breakdown in a number of mental functions, including those involved in emotion, thought and cognition. There is, however, significant heterogeneity in the etiopathology and symptomatology of this disorder; as a result it has been argued that it may not be a single disorder or disease entity.[1] Instead it is believed that selective etiological bases and associated pathophysiology underpin schizophrenia in different individuals.[2,3] A current challenge is to deconstruct the disorder based on these underlying factors. This would consequently lead to a greater understanding of the pathophysiology that characterizes homogenous subgroups and would aid in the development of more selective therapeutics. However, the ability to deconstruct such a heterogeneous syndrome into different etiological underpinnings is difficult, if not impossible, in a human population. To this end, the use of animal models that conceptualize specific etiopathological bases of this disorder so that the underlying physiological changes can be identified is needed to advance our understanding of schizophrenia. Etiological studies have reported an increased risk for schizophrenia development as a result of maternal immune activation (MIA), with it being estimated that more than 30% of schizophrenia cases are associated with this event.[4] This can be modeled in rodents as a means to examine how *in utero* environmental challenge leads to neuroanatomical alterations that underpin this increased risk.[5]

Effective integration of neural activity relies on precise temporal coordination, or synchrony, of neural oscillations.[6,7] Abnormal neural synchronisation has been observed in individuals with schizophrenia across a broad range of frequency bands.[8–11] This includes effects in first-episode, unmedicated schizophrenia patients[12] and their first-degree relatives[13] suggesting that it is not a result of medication and may represent an endophenotype for the disorder.[14] This aberrant synchrony and the resultant disruption in integrative processes may contribute to the underlying pathophysiology of schizophrenia.[14] Using the polyinosinic-polycytidylic acid induced MIA model, we have previously shown that synchrony is reduced between the dorsal hippocampus (HPC) and medial prefrontal cortex (mPFC),[15] two brain regions prominent in schizophrenia neuropathology.[16,17] However, a critical question is whether this abnormal synchrony is specific to these particular pathways and networks. Clarification would facilitate an understanding of the pathophysiology that is specifically associated with MIA.

The HPC has consistently been implicated in schizophrenia, with both functional and structural disturbance being observed.[17,18] Many of these changes have also been reported in animal models, including those involving MIA.[19,20] Much previous work in this area has, however, either tended to focus on the HPC as a whole

[1]Department of Psychology, University of Otago, Dunedin, New Zealand; [2]Brain Health Research Centre, University of Otago, Dunedin, New Zealand and [3]Department of Anatomy, University of Otago, Dunedin, New Zealand. Correspondence: Dr DK Bilkey, Department of Psychology, University of Otago, PO Box 56, Dunedin 9054, New Zealand. E-mail: dbilkey@psy.otago.ac.nz
[4]These authors contributed equally to this paper.
Received 26 February 2014; revised 15 June 2014; accepted 16 June 2014

or has focused on the ventral or dorsal regions alone. A more discriminatory approach may be worthwhile, as the dorsal and ventral poles of the HPC are functionally distinct and possess markedly different connectivity with downstream cortical targets including the mPFC.[21] Our previous work, for example, focused on MIA-induced reductions in dorsal HPC–mPFC synchrony. However, it is the ventral HPC that is directly connected to the mPFC,[22] whereas the dorsal HPC–mPFC connection is polysynaptic. Furthermore, while reports on hippocampal pathology in schizophrenia do not generally differentiate between ventral and dorsal regions as noted, specific disruption of the ventral HPC has been reported in some studies.[23,24] We hypothesized, therefore, that an MIA manipulation would generate a greater deficit in coherence between ventral HPC–mPFC than between dorsal HPC–mPFC due to the differential connectivity between these regions.

The HPC has previously been implicated in the generation and modulation of local and long-range oscillatory activity.[25,26] Gamma-aminobutyric acid (GABA)-ergic interneurons have an important role in this process,[27] and as there is much evidence that indicates alterations in this neurotransmitter system in schizophrenia,[28] it is possible that the molecular basis of aberrant synchrony in both schizophrenia and the MIA model may lie in altered GABAergic signaling.[29] Of particular interest are parvalbumin (PV)-expressing GABAergic interneurons, which have been shown to have an important role in modulating neural synchrony.[30–33] There are descriptions of abnormalities in PV-positive cells in schizophrenia, including reduced PV cell numbers,[34] or reduced PV or glutamic decarboxylase (GAD67) expression within interneurons in the absence of neuronal loss.[30] Given a potential relationship between synchrony and inhibition, we predicted that any difference in synchrony that we might observe between ventral and dorsal HPC and the mPFC in the MIA model would be associated with selective changes in GAD67 expression in PV interneurons.

To test these predictions we assessed the long-range coherence of electroencephalogram (EEG) recorded in the dorsal and ventral regions of the HPC with that recorded in the mPFC. In addition, we examined GAD67 expression levels within the ventral and dorsal HPC both globally and within PV-positive interneurons, followed by stereological analysis of PV cell number within these structures. Contrary to our initial hypothesis, reduced coherence was selective to mPFC-dorsal HPC coupling. GAD67 expression was also selectively reduced, both globally and within PV-positive interneurons, in the dorsal HPC relative to the ventral HPC, in the absence of PV-positive neuronal loss, supporting our prediction that coherence and GAD67 changes would be associated.

MATERIALS AND METHODS

All procedures were performed in accordance with ethical guidelines of the University of Otago Ethics Committee.

Animals

Female Sprague–Dawley rats were mated at 3 months. On gestational day 15, under halothane anesthesia, experimental-group dams were injected with a single dose of polyinosinic:polycytidylic acid (4.0 mg kg^{-1}, intravenous; Sigma, Auckland, New Zealand) dissolved in saline, while control dams received saline injection.[15,35] Separate cohorts of the adult (at least three months old) male offspring of these animals were used for the electrophysiology and anatomical procedures. Animals used for the western blot analysis were independent from those used in the immunohistochemical-based analyses. Some animals contributed to both immunofluorescence and stereology procedures.

Electrophysiological recordings

Surgery and electrode implantation. Adult animals (11 MIA from 8 litters and 10 control from 9 litters) were anesthetized with ketamine (75 mg kg^{-1}, intraperitoneal) and domitor (0.5 mg kg^{-1}, intraperitoneal), and chronically implanted with recording electrodes (127-μm diameter formvar-coated, nichrome wires; California Fine Wire, Grover Beach, CA, USA), into the left hemisphere based on coordinates from Paxinos and Watson.[36] The mPFC electrode targeted the prelimbic cortex (from bregma: +3.2 mm anterior-posterior; −0.6 mm medial-lateral; 3.2 mm ventral to dura). Two hippocampal EEG electrodes were implanted targeting the CA1 regions of the dorsal HPC (−3.8 mm anterior-posterior; −2.5 mm medial-lateral; 2.5 mm ventral to dura) and the ventral HPC (−5.6 mm anterior-posterior; −3.5 mm medial-lateral; angled 11° lateral from the midline, 6.6 mm ventral to dura). Following two weeks recovery, animals were reduced to ~85% of their free-feeding weight to optimize behavioral procedures.

Electrophysiological recordings. Depth EEG was recorded from the three regions using the dacqUSB multichannel recording system (Axona, St Albans, UK). EEG signals were buffered via a Field Effect Transistor source-follower mounted to the headstage, referenced to a skull screw, low-pass filtered at 600 Hz, and sampled at 4800 Hz. The animal's head position was monitored by a ceiling-mounted video camera connected to a tracking system that monitored infrared LEDs mounted on the head stage (sampled at 50 Hz).

Recording apparatus and procedure. The experimental chamber was a black, plastic, circular tub (74-cm diameter) with a wall height of 56 cm. The room was lit by a low-level light source located at one side of the room. This was not directly visible to the animal while in the apparatus. Animals were handled for 2 days before experimentation and habituated for 2 × 20 min sessions within the environment for 2 days before their first recording. Two 10-min recordings were then obtained each day (AM/PM) while animals foraged in the open-field environment.

Data analysis

Power spectral analysis: Power spectral density analyses of regional EEG were conducted using Welch's modified method of spectral estimation (Matlab, pwelch(*x*)) using a discrete Fourier transform with a 9600-point sample, moving hamming window, giving a resolution of 0.5 Hz. The power spectral density was normalized by fitting an exponential curve using the least squares method.[15,37] The difference between the fitted curve and the power spectral density was retained and the amplitude and frequency of the peaks in this difference curve measured in the delta (2–4 Hz), theta (4–12 Hz), beta (12–30 Hz) and gamma (low 30–48 Hz and high 52–100 Hz) frequency bands. This procedure was conducted using an automated Matlab routine and results within each frequency band were compared between the control and MIA animals using *t*-tests.

Coherence analysis: Coherence, a measure of the covariation between two EEG signals as a function of frequency, was calculated using the Matlab function *mscohere* (Mathworks, Natick, MA, USA) as previously described.[15] A frequency resolution of 0.5 Hz was available. The magnitude of coherence between regions was extracted for each frequency band and compared. Peak coherence values within each band were averaged across all recordings for each animal, providing a mean coherence value for each animal within each frequency band. Upon completion of electrophysiological recordings, histological procedures were used to verify electrode placements.[15]

Western blotting

Animals (MIA $n = 7$, control $n = 7$; from three litters per condition) were anesthetized with halothane before removal and dissection of dorsal and ventral CA1 and the mPFC from the left and right hemisphere of each animal. Tissue was flash-frozen and stored at −80 °C until processing. Total protein extracts were prepared as per Williams *et al*.[38] Dorsal and ventral HPC and mPFC protein extracts from each hemisphere (10 μg) were separated by SDS–polyacrylamide gel electrophoresis (9%) and transferred to a nitrocellulose membrane (Schleicher and Schuell, GE Healthcare, Auckland, New Zealand). Membranes were probed with an antibody recognizing GAD67 (1:5000, Sigma, Saint Louis, MO, USA) and tubulin (1:5000, Abcam, Cambridge, UK). Antibody binding was visulized using peroxidase-conjugated secondary antibodies (Sigma) and enhanced chemiluminescence (Pierce: ThermoFisher, Auckland, New Zealand). Resulting X-ray films were quantified by densitometry.[39]

Data analysis. GAD67 protein expression was normalized relative to tubulin in the same sample. All data were generated from within-membrane comparisons and expressed relative to averages determined

for tubulin-normalized controls. For the HPC, a mixed-model analysis of variance (ANOVA) was used to assess differences in protein expression between groups and across regions. Differences within the mPFC were assessed using *t*-tests.

Dual-label Immunofluorescence

Animals (all from independent litters; MIA $n=7$, control $n=7$) were anesthetized with halothane and transcardially perfused with 200 ml of phosphate-buffered saline, followed by 200 ml of 4% paraformaldehyde. The brains were removed and post-fixed in 4% paraformaldehyde for 12 h, and then transferred to a 20% sucrose cryoprotectant solution until sectioning.

For each animal, free-floating (40 μm) sections of the left dorsal (−2.4 to −4.20 mm posterior to bregma) and ventral HPC (−4.80 to −6.00 mm posterior to bregma) were cut on a freezing microtome. For each animal, 2–6 sections at 590 μm and 300 μm intervals for the dorsal and ventral HPC, respectively were randomly selected and assayed for PV and GAD67 expression. Sections from MIA and matched controls were processed within the same wells to control for staining variations. Sections were probed with antibodies recognizing parvalbumin (Abcam, 1:2000) and anti-GAD67 (1:2000, Millipore, Temecula, CA, USA). Antibodies were visualized using Alexa 488 goat anti-mouse and Alexa 555 goat anti-rabbit (GAD and PV respectively; both 1:500, Invitrogen, Camarillo, CA, USA) conjugated secondary antibodies.

Immunofluorescence was observed using a confocal microscope (Carl Zeiss 710, Macquarie Park, NSW, Australia) with a ×10 objective lens. Settings were kept consistent throughout the experiment. Z-stacks comprising 10×10.5 μm sections with an interval of 5.26 μm were taken throughout the section and converted to max projections. ImageJ (NIH) was used to select PV immunoreactive cell bodies in the pyramidal cell and stratum oriens layers within the left hemisphere. Within both channels, mean pixel intensity within each PV cell body >100 pixels was determined. No less than 15 cells from the ventral and 17 cells from the dorsal hippocampus were analyzed for each animal with an average of 54 and 50 cells analyzed for each region, respectively.

Data analysis. To control for technical variability, all data were generated by within-batch comparison of normalized values for MIA and controls; batches consisted of matched control and MIA animals processed at the same time. Data for all cells were expressed relative to the average value across all cells within each batch, and then an overall average for each animal determined. A mixed-model design ANOVA was used to compare average intensity between MIA and control animals across regions.

Stereology

Animals (MIA $n=7$, control $n=7$; from seven and six litters, respectively) were perfused and brains extracted as described above for the dual-label immunofluorescence. A sliding microtome was used to cut free-floating (30 μm) sections of the dorsal (−2.4 to −4.20 mm posterior to bregma) and ventral HPC (−4.80 to −6.00 mm posterior to bregma). Every ninth section of the left hemisphere was analyzed, giving an average of seven and five sections from each animal for the dorsal and ventral HPC, respectively.

Sections were stained for PV immunoreactivity as described above except that the antibody was visualized using VectorStain elite ABC kit (Vector Labs, Burlingame, CA, USA) and developed using DAB-peroxidase. Cell counts within the entire dorsal and ventral CA1 region were visualized using a X20 objective and quantified using Stereo-Investigator software (version 10.2.1.1; MBF Bioscience, Williston, VT, USA).

Data analysis. Group estimations of PV cell populations were averaged and differences between groups across regions were analyzed using a mixed-model ANOVA. Group averages for the coefficient of error and volume were analyzed using *t*-tests.

RESULTS

MIA selectively disrupts long-range synchrony between mPFC and dorsal HPC

To determine whether there were region-specific EEG effects, coherence was measured between the mPFC and the dorsal or ventral HPC in MIA animals ($n=11$; from 115 EEG recordings) and litter-matched controls ($n=10$; from 100 EEG recordings). Analysis of the mean peak coherence revealed a significant reduction between the mPFC and the dorsal HPC in MIA animals compared with controls (Figure 1a). This broad-spectrum effect occurred from the delta to the high-gamma frequency bands (delta,

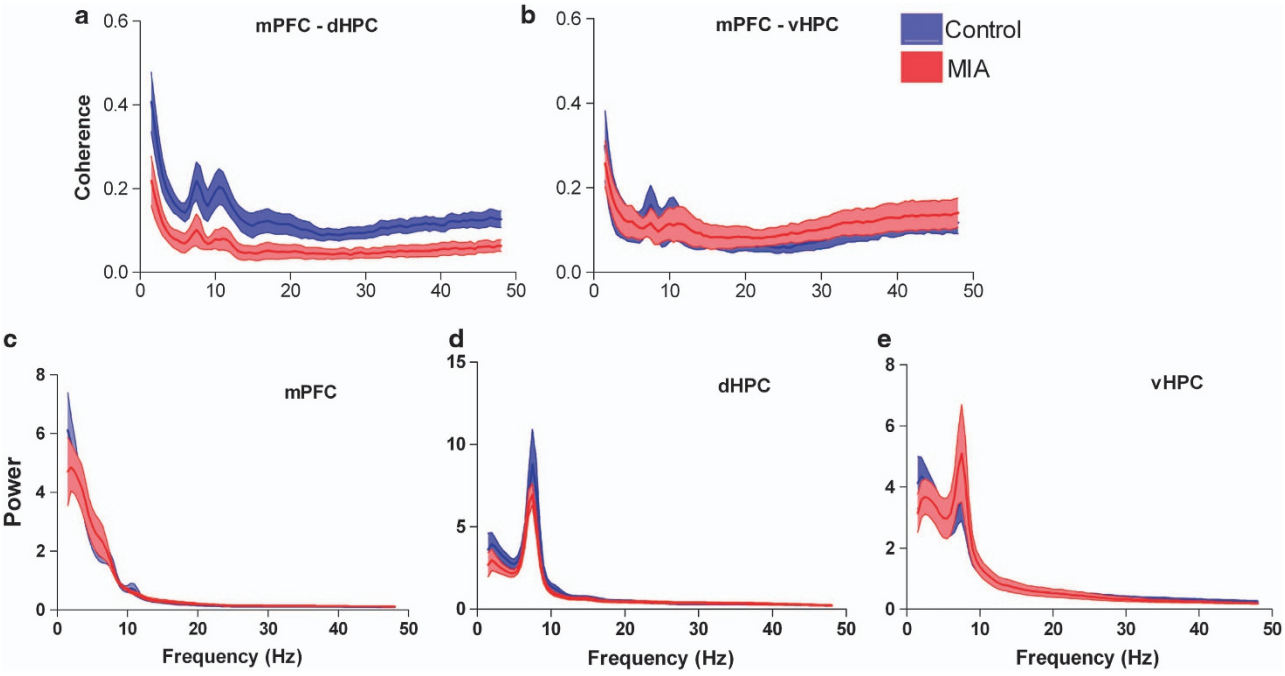

Figure 1. (**a**, **b**) Coherence spectrogram (mean ± s.e.m.) of EEG simultaneously recorded from (**a**) dorsal HPC and mPFC illustrating a significant reduction in coherence in the MIA animals between these brain regions, (**b**) no difference in coherence was noted between ventral HPC and mPFC. (**c**–**e**) Mean (± s.e.m.) power spectral density plots reveal MIA animals have similar power across all frequency bands in (**c**) mPFC, (**d**) dorsal HPC and (**e**) ventral HPC. EEG, electroencephalogram; HPC, hippocampus; MIA, maternal immune activation; mPFC, medial prefrontal cortex.

$t_{19} = 2.261$, $P = 0.036$; theta $t_{19} = 3.401$, $P = 0.003$; beta, $t_{18} = 2.439$, $P = 0.026$; low gamma, $t_{13} = 2.716$, $P = 0.018$; and high-gamma, $t_{16} = 2.429$, $P = 0.027$). There were no between-group differences in terms of the frequency at which peak coherence occurred for any of the frequency bands (all $P > 0.2$). In contrast, the MIA manipulation had no effect on either the magnitude or the frequency of peak coherence when coherence between mPFC and the ventral HPC was measured for any of the bands (Figure 1b). There was also a significant reduction in coherence between the dorsal and ventral HPC in the delta frequency band ($t_{19} = 2.502$, $P = 0.022$) in MIA animals. A two-way, repeated measures ANOVA revealed a significant group by region interaction in the theta frequency band ($F_{1,19} = 5.039$, $P = 0.037$) indicating that coherence to mPFC differed between the dorsal and ventral hippocampus as a result of the MIA manipulation.

Disrupted long-range synchrony is not explained by disrupted local power

The amplitude of the normalized local power spectra did not differ between MIA and control offspring in the mPFC, dorsal HPC or ventral HPC within any of the frequency bands investigated, with the exception of the delta band where there was a significant reduction in power in the MIA ventral HPC ($t_{19} = 2.120$, $P = 0.047$; Figures 1c–e). The frequency at which the peak normalized power amplitude occurred did not differ between groups in any of the three regions, except that the frequency of peak delta power in the mPFC was significantly higher for MIA than control animals (MIA 2.83 ± 0.10 Hz; control $2.52 \pm 0.10.6$ Hz; $t_{19} = 2.150$, $P = 0.045$).

MIA animals exhibit changes in GAD67 expression within the dorsal HPC

To examine whether our observed changes in long-range synchrony were associated with changes in GAD67 expression, we analyzed GAD67 levels within the mPFC and dorsal and ventral HPC in both hemispheres by western blot. A significant group by region interaction was observed in the left hemisphere ($F_{1,12} = 10.379$, $P = 0.007$) as well as a significant main effect of region ($F_{1,12} = 10.379$, $P = 0.007$) in the absence of a group main effect ($P > 0.52$). The significant interaction indicates that the MIA effects on GAD67 differed between the left dorsal and ventral HPC. This was due to a decrease in immunoreactivity in the dorsal HPC and an increase in the ventral HPC in MIA animals relative to controls (Figures 2a and di). Analysis of the right hemisphere did not reveal a significant interaction ($P > 0.59$), or any group ($P > 0.91$) or region ($P > 0.59$) main effects (Figures 2b and dii). Analysis of GAD67 density levels within the mPFC using two-tailed independent sample *t*-tests also failed to reach significance for

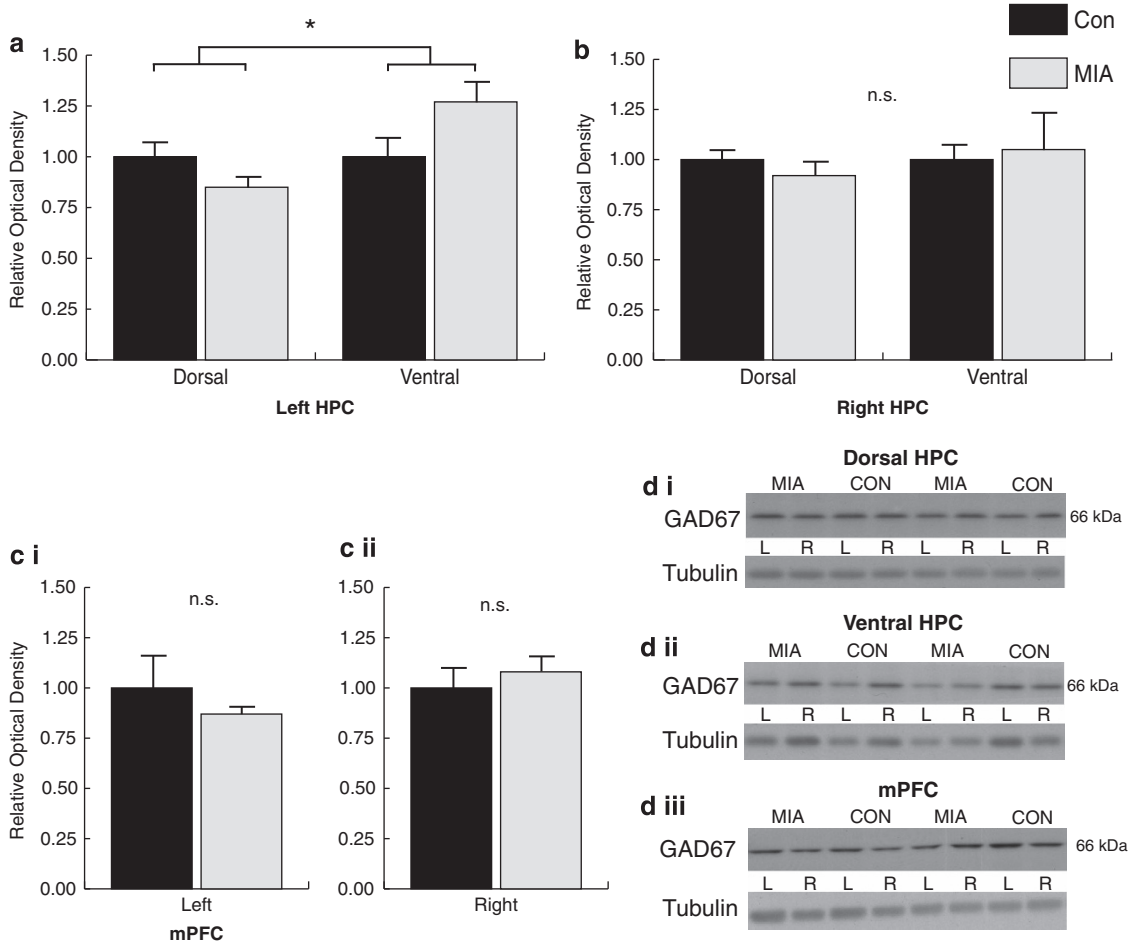

Figure 2. Analysis of GAD67 immunoreactivity as a function of MIA. (**a**) Western blot analysis revealed a decrease in GAD67 expression in the left dorsal HPC relative to the ventral. Analysis of the right HPC (**b**) and the mPFC (left **c**i, right **c**ii) failed to produce significant effects. (**d**) Representative gels illustrating GAD67 and tubulin immunoreactivity within the dorsal HPC (i), ventral HPC (ii) and mPFC (iii). GAD67, glutamic decarboxylase; HPC, hippocampus; MIA, maternal immune activation; mPFC, medial prefrontal cortex. *Significant ($P < 0.05$) group by region interaction, n.s. (not significant).

either hemisphere: left $P > 0.39$ (Figures 2ci and diii); right, $P > 0.50$ (Figures 2cii and diii).

Reduced GAD67 protein expression is observed within PV-positive interneurons in the absence of neuronal loss

Given the role of PV-positive interneurons in influencing neuronal synchrony, we next investigated whether the pattern of altered GAD67 expression observed in the left ventral and dorsal HPC was apparent within PV-positive interneurons within the same hemisphere. A mixed-model ANOVA revealed a significant group by region interaction ($F_{1,12} = 4.932$, $P < 0.046$) for GAD67 immunoreactivity but not PV (Figure 3a–c). This indicated that the intensity of GAD67 expression within PV-positive cells in the dorsal HPC was selectively reduced relative to ventral HPC expression in MIA animals compared with controls. This occurred in the absence of any other main effects (region $P = 0.63$, group $P = 0.34$) and analysis of PV fluorescence intensity across the ventral and dorsal HPC also failed to reveal any effects (region $P = 0.77$, group $P = 0.416$, region × group $P = 0.31$).

Finally, we examined whether PV neuronal numbers were reduced in the dorsal and ventral HPC regions of MIA animals relative to controls. A stereological analysis of PV-positive cell numbers within the left dorsal and ventral HPC using the optical fractionator method revealed no significant group differences with similar group estimates for PV cell number, coefficient of error and volume analyzed (all $P > 0.05$; Table 1), indicating that the GAD67 effects were not secondary to PV cell loss.

DISCUSSION

Synchronous neural action underpins the effective integration of activity in brain networks, and GABAergic interneurons have a major role in these processes.[33] Considerable evidence points to a dysfunction in GABAergic neurotransmission in individuals with

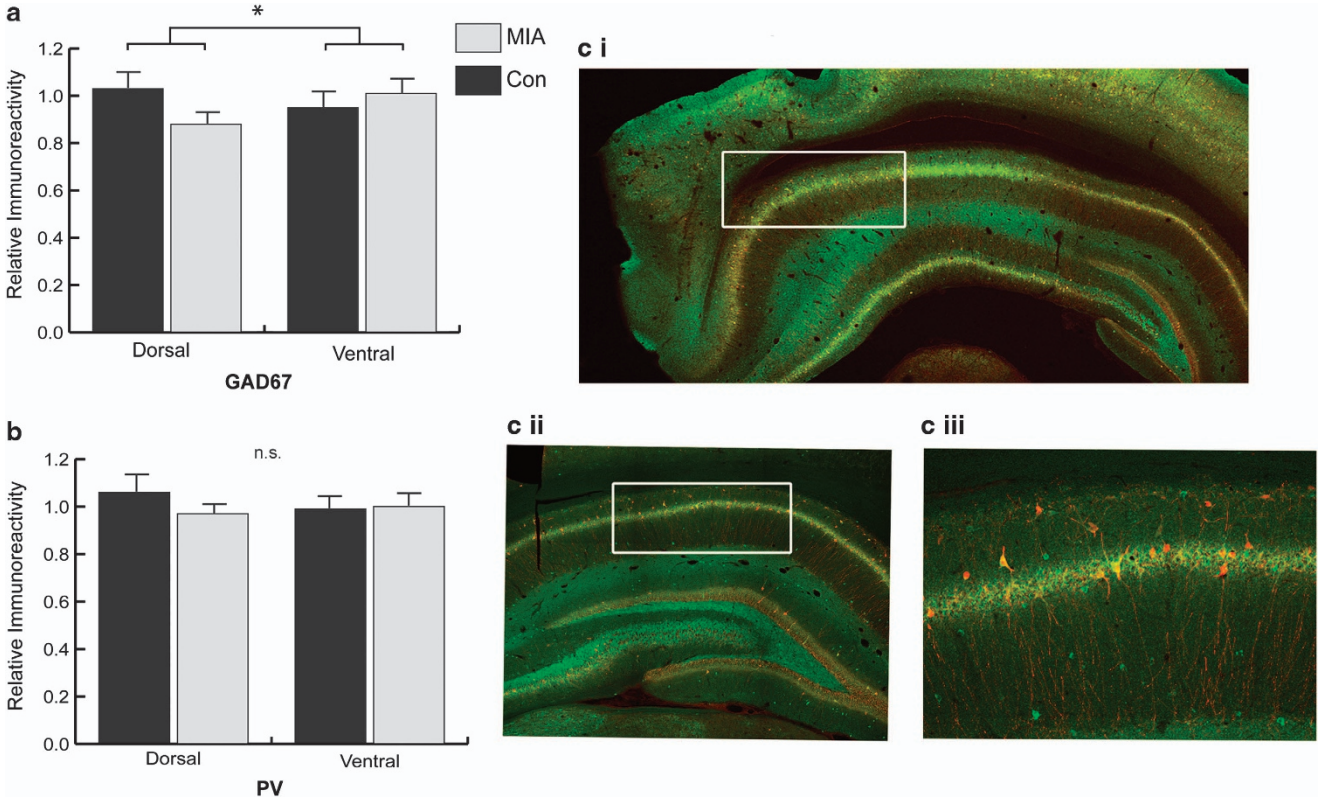

Figure 3. Analysis of PV immunoreactivity within PV-positive cells. (**a**) Analysis within the dorsal HPC revealed a reduction in GAD67 immunoreactivity relative to the ventral for MIA animals. (**b**) Analysis of PV immunoreactivity within the same dorsal HPC cells failed to produce an effect. (**ci**–iii) Micrographs illustrating immunohistochemistry staining of GAD67 (green) and PV (red). (**c**) The typical region of analysis within the ventral (i) and dorsal (ii) HPC depicted in white. (**ci**ii) Increased magnification of the immunostaining showing double labeling GAD67+PV (yellow–red), and single GAD67 only (green) cells. GAD67, glutamic decarboxylase; HPC, hippocampus; MIA, maternal immune activation; PV, parvalbumin. *Significant ($P < 0.05$) group by region interaction, n.s. (not significant).

Table 1. Summary of PV-positive cell estimates, CE and volume in the dorsal and ventral HPC of MIA and control (CON) animals

Dorsal CA1				*Ventral CA1*			
Treatment	*No. of cells*	*CE*	*Volume* ($\times 10^6\ \mu m^{-3}$)	*Treatment*	*No. of cells*	*CE*	*Volume* ($\times 10^6\ \mu m^{-3}$)
MIA	4565 ± 669	0.116 ± 0.016	2860.44 ± 216.07	MIA	4385 ± 319	0.109 ± 0.004	3302.05 ± 346.72
CON	4070 ± 532	0.113 ± 0.005	2607.00 ± 123.48	CON	5527 ± 918	0.101 ± 0.016	3562.01 ± 376.97

Abbreviations: CE, coefficient of error; HPC, hippocampus; MIA, maternal immune activation; PV, parvalbumin.

schizophrenia, and these deficits may underlie the abnormal synchrony evident in the disorder.[29] Our data provide new evidence of an association between neural synchrony and GAD67 expression. These data extend our previous finding of reduced long-range communication between the HPC and the mPFC in the MIA model of a schizophrenia risk factor,[15] by demonstrating that this effect is specific to connections between the mPFC and dorsal HPC. Significantly, GAD67 protein expression was reduced in dorsal relative to ventral HPC when measured in both a global and PV-interneuron specific manner. These findings provide the first evidence of an association between long-range synchronisation processes and GAD67 expression, potentially linking reduced GABAergic neurotransmission in the dorsal HPC with the long-range breakdown in synchrony between this region and the prefrontal cortex.

Synchronisation of local and long-range neural networks requires GABA-mediated inhibition of pyramidal cells and the associated phasic regulation of excitation. Through dense perisomatic and dendritic innervation of glutamatergic neurons, GABAergic interneurons are able to control network activity and produce synchronous oscillatory activity within various frequency bands.[40] For example, oscillations within the gamma frequency range are driven by activity in GABAergic inhibitory systems and associated with local synchronisation;[41,42] whereas lower frequency activity, for example, within the theta range, has been linked to long-range communication processes[43] and is also modulated by GABA.[44] Previous studies have linked aberrant local oscillatory activity in schizophrenia with a subclass of GABAergic interneurons containing the calcium-binding protein PV. Specifically, alterations in PV cell number have been associated with disrupted local oscillatory activity in genetic, developmental and acute models of psychiatric illness.[45,46] While our results are also linked to changes in PV-positive interneurons, our critical finding was that these changes are linked to long-range neuronal synchrony and appear to be driven by a reduction in the density of GAD67 within PV-positive interneurons rather than PV cell loss. Selective suppression of inhibition in PV-positive interneurons has previously been shown to decrease theta rhythm activity,[47] an effect that is likely to directly impair long-range communication[43] and also alter the coupling between theta and gamma activity.[47] Our findings are consistent with previous studies showing a lateralized disruption of the hippocampal GABAergic system in schizophrenia,[48] that administration of polyinosinic-polycytidylic acid during mid-gestation failed to alter PV-positive cell number in the HPC,[49] and that reduced GAD67 expression was observed in the absence of neuronal loss in an animal model of schizophrenia and in postmortem schizophrenic tissue.[30,50,51] Overall, we observed reduced GAD67 expression within the dorsal HPC that was further localized to PV-positive cell types. It is possible that GAD67 expression was also reduced in other interneuronal subtypes such as those that express calbindin, calretinin or somatostatin. However, given the known role of PV-positive interneurons in mediating synchrony,[30–33] it is likely that reduced GAD67 expression specific to PV-positive cells may have underpinned the altered activity observed here. This could by clarified in future studies by utilizing a lentiviral-based RNA interfering strategy to induce a modest reduction in dorsal HPC GAD67 expression within PV-positive cells, followed by analyses of neuronal synchrony. Of further interest for subsequent studies is the mechanism within the MIA model that caused region-specific alterations in GAD67 expression within the HPC. Previous research has shown that GAD67 expression is regulated by neuronal activity,[52] thus the reduced GAD67 expression within PV-positive neurons in the dorsal HPC reported here may be driven by aberrant inputs to PV neurons either locally or from some third-party region.

Direct monosynaptic connections link the ventral HPC to the mPFC, whereas the dorsal HPC and mPFC are indirectly linked via intermediary regions. We predicted a greater reduction in coherence between the directly connected brain regions compared with those that were indirectly linked. Instead, we observed a reduction in synchrony only between the dorsal HPC and mPFC. The reduction in synchrony and associated changes in GAD67 expression observed in this study may therefore reflect dysfunction in one or more of the intermediary regions. For example, the nucleus reuniens possesses unique reciprocal connectivity enabling it to coordinate the activity of both the mPFC and HPC.[22] Other differences in afferent and efferent projections of the dorsal and ventral subregions of the hippocampal formation may also contribute to the altered synchrony. The selective loss of synchrony observed within the dorsal hippocampus has the potential to impact on spatial memory, as this portion of the rat hippocampus has been shown to have an important role in this function.[53,54] This may account for the spatial memory deficits, for example, observed in MIA animals[55] and, as the fundamental organization of hippocampal connectivity is generally consistent between rats and primates,[54] similar problems may occur in individuals with schizophrenia,[56] if the analogous region of the human hippocampus (posterior hippocampus) is affected. Overall, despite our initial hypothesis not being supported, our results are consistent with some previous findings in the schizophrenia literature where HPC alterations have been specifically localized to the posterior (dorsal) HPC rather than the ventral (anterior) region.[57,58] The experiments described here revealed that MIA-induced changes occurred in the left hemisphere of the brain. EEG recordings were only conducted for this hemisphere, as were the immunofluorescence and stereology analyses, so we do not know what effects might be evident in the right hemisphere. This is worthy of further investigation, as the results of the western blots, which were conducted separately for tissue from each hemisphere, indicated a selective left-sided effect. This may be relevant to schizophrenia as a number of studies[59] have suggested that alterations in hemispheric asymmetry, including in one example, selective reductions in inhibition in the left hemisphere,[60] may be important in the disorder.

In the present study, it is notable that the differential long-range coupling between brain regions in MIA animals was not explained by disrupted local oscillatory activity in any of the three regions. A key question, therefore, is how changes in GAD67 expression in the dorsal HPC affect long-range synchronisation but not local oscillatory mechanisms? One possibility is that long-range polysynaptic synchrony is less robust and is consequently affected by the relatively subtle changes in inhibitory interneurons observed in the present study. Alternatively, changes in GAD67 expression may be selective for a particular subpopulation of interneurons that is influenced by extra-hippocampal afferents to a greater extent than local circuitry. Regardless of the specific mechanism, however, these findings provide an important link between regional alterations in GAD67 expression and the selective disruptions in long-range synchrony that result from exposure to the maternal immune response. Thus, the results help to elucidate the mechanisms characteristic of the *in utero* MIA event that contribute to increased risk for schizophrenia.

CONFLICT OF INTEREST

The authors declare no conflict of interest.

ACKNOWLEDGMENTS

This research was supported by grants from the Health Research Council of New Zealand and the Marsden Fund. We thank Sara Illingworth, James McKearney, Shane Ohline, Rehutai Smith-Iri and Diane Guévremont for their technical assistance.

REFERENCES

1 Tandon R, Nasrallah MS, Keshavan MS. Schizophrenia, 'just the facts' 4. Clinical features and conceptualization. *Schizophr Res* 2009; **110**: 1–23.
2 Keller WR, Fischer BA, Carpenter WT Jr. Revisiting the diagnosis of schizophrenia: where have we been and where are we going? *CNS NeurosciTher* 2011; **17**: 83–88.
3 Thanker GK. Schizophrenia endophenotypes as treatment targets. *Expert Opin Ther Targets* 2007; **11**: 1189–11206.
4 Brown AS, Derkits EJ. Prenatal infection and schizophrenia: a review of epidemiologic and translational studies. *Am J Psych* 2010; **167**: 261–280.
5 Meyer U, Feldon J. To poly(I:C) or not to poly(I:C): Advancing preclinical schizophrenia research through the use of prenatial immune activation models. *Neuropharmacology* 2012; **62**: 1308–1321.
6 Singer W. Neuronal synchrony: a versatile code for the definition of relations? *Neuron* 1999; **24**: 49–65, 111-25.
7 Buzsaki G, Draguhn A. Neuronal oscillations in cortical networks. *Science* 2004; **304**: 1926–1929.
8 Uhlhaas PJ, Linden DE, Singer W, Haenschel C, Linder M, Maurer K *et al.* Dysfunctional Long-Range Coordination of Neural Activity during Gestalt Perception in Schizophrenia. *J Neurosci* 2006; **26**: 8168–8175.
9 Ford JM, Roach BJ, Faustman WO, Mathalon DH. Synch before you speak: auditory hallucinations in schizophrenia. *Am J Psych* 2007; **164**: 458–466.
10 Ford JM, Mathalon DH, Whitfield S, Faustman WO, Roth WT. Reduced communication between frontal and temporal lobes during talking in schizophrenia. *Biol Psych* 2002; **51**: 485–492.
11 Tauscher J, Fischer P, Neumeister A, Rappelsberger P, Kasper S. Low frontal electroencephalographic coherence in neuroleptic-free schizophrenic patients. *Biol Psych* 1998; **44**: 438–447.
12 Koenig T, Lehmann D, Saito N, Kuginuki T, Kinoshita T, Koukkou M. Decreased functional connectivity of EEG theta-frequency activity in first-episode, neuroleptic-naive patients with schizophrenia: preliminary results. *Schizophr Res* 2001; **50**: 55–60.
13 Hong LE, Summerfelt A, McMahon R, Adami H, Francis G, Elliott A *et al.* Evoked gamma band synchronization and the liability for schizophrenia. *Schizophr Res* 2004; **70**: 293–302.
14 Uhlhaas PJ, Singer W. Abnormal neural oscillations and synchrony in schizophrenia. *Nat Rev Neurosci* 2010; **11**: 100–113.
15 Dickerson DD, Wolff AR, Bilkey DK. Abnormal long-range neural synchrony in a maternal immune activation animal model of schizophrenia. *J Neurosci* 2010; **30**: 12424–12431.
16 Ellison-Wright I, Bullmore E. Anatomy of bipolar disorder and schizophrenia: a meta-analysis. *Schizophr Res* 2010; **117**: 1–12.
17 Harrison PJ. The hippocampus in schizophrenia: a review of the neuropathological evidence and its pathophysiological implications. *Psychopharmacology (Berl)* 2004; **174**: 151–162.
18 Boos H. Brain volumes in relatives of patients with schizophrenia. *JAMA Psychiatry* 2007; **64**: 297–304.
19 Savanthrapadian S, Wolff AR, Logan BJ, Eckert MJ, Bilkey DK, Abraham WC. Enhanced hippocampal neuronal excitability and LTP persistence associated with reduced behavioral flexibility in the maternal immune activation model of schizophrenia. *Hippocampus* 2013; **23**: 1395–1409.
20 Ito HY, Smith SE, Hsiao E, Patterson PH. Maternal immune activation alters nonspatial information processing in the hippocampus of the adult offspring. *Brain Behav Immun* 2010; **24**: 930–941.
21 Fanselow MS, Dong HW. Are the dorsal and ventral hippocampus functionally distinct structures? *Neuron* 2010; **65**: 7–19.
22 Di Prisco GV, Vertes RP. Excitatory actions of the ventral midline thalamus (rhomboid/reuniens) on the medial prefrontal cortex in the rat. *Synapse* 2006; **60**: 45–55.
23 Malaspina D, Storer S, Furman V, Esser P, Printz D, Berman A *et al.* SPECT study of visual fixation in schizophrenia and comparison subjects. *Biol Psychiatry* 1999; **46**: 89–93.
24 Lipska BK, Swerdlow NR, Geyer MA, Jaskiw GE, Braff DL, Weinberger DR. Neonatal excitotoxic hippocampal damage in rats causes post-pubertal changes in prepulse inhibition of startle and its disruption by apomorphine. *Psychopharmacology (Berl)* 1995; **122**: 35–43.
25 Csicsvari J, Jamieson B, Wise KD, Buzsaki G. Mechanisms of gamma oscillations in the hippocampus of the behaving rat. *Neuron* 2003; **37**: 311–322.
26 Buzsaki G. Theta oscillations in the hippocampus. *Neuron* 2002; **33**: 325–340.
27 Bartos M, Vida I, Jonas P. Synaptic mechanisms of synchronized gamma oscillations in inhibitory interneuron networks. *Nat Rev Neurosci* 2007; **8**: 45–56.
28 Akbarian S, Huang HS. Molecular and cellular mechanisms of altered GAD1/GAD67 expression in schizophrenia and related disorders. *Brain Res Rev* 2006; **52**: 293–304.
29 Lewis DA, Fish KN, Arion D, Gonzalez-Burgos G. Perisomatic inhibition and cortical circuit dysfunction in schizophrenia. *Curr Opin Neurobiol* 2011; **21**: 866–872.
30 Hoshimoto T, Volk DW, Eggan SM, Mirnics K, Pierri JN, Sun Z *et al.* Gene expression deficits in a subclass of GABA neurons in the prefrontal cortex of subjects with schizophrenia. *J Neurosci* 2003; **23**: 6315–6326.
31 Cardin JA, Carlen M, Meletis K, Ulf K, Zhang F, Deisseroth K *et al.* Driving fast-spiking cells induces gamma rhythm and controls sensory responses. *Nature* 2009; **459**: 663–667.
32 Carlen M, Meletis K, Siegle JH. A critical role for NMDA receptors in parvalbumin interneurons for gamma rhythm induction and behavior. *Mol Psychiatry* 2012; **17**: 537–548.
33 Sohal VS, Zhang F, Yizhar O, Deisseroth K. Parvalbumin neurons and gamma rhythms enhance cortical circuit performance. *Nature* 2009; **459**: 698–702.
34 Sakai T, Oshima A, Nozaki Y, Ida I, Haga C, Akiyama H *et al.* Changes in density of calcium binding protein immunoreactive GABAergic neurons in prefrontal cortex in schizophrenia and bipolar disorder. *Neuropathology* 2008; **28**: 143–150.
35 Wolff AR, Bilkey DK. Immune activation during mid-gestation disrupts sensorimotor gating in rat offspring. *Behav Brain Res* 2008; **190**: 156–159.
36 Paxinos G, Watson C. *The Rat Brain in Stereotaxic Coordinates*. 4th Edn, Academic Press: San Diego, CA, USA, 1998.
37 Russell NA, Horii A, Smith PF, Darlington CL, Bilkey DK. Lesions of the vestibular system disrupt hippocampal theta rhythm in the rat. *J Neurophysiol* 2006; **96**: 4–14.
38 Williams JM, Mason-Parker SE, Abraham WC, Tate WP. Biphasic changes in the levels of N-methyl-D-aspartate receptor-2 subunits correlate with the induction and persistence of long-term potentiation. *Brain Res Mol Brain Res* 1998; **60**: 21–27.
39 Williams JM, Guevremount D, Mason-Parker SE, Luxman C, Tate WP, Abraham WC. Differential trafficking of AMPA and NMDA receptors during long-term potentiation in awake adult animals. *J Neurosci* 2007; **27**: 14171–14178.
40 Cobb SR, Buhl EH, Halasy K, Paulsen O, Somogyi P. Synchronization of neuronal activity in hippocampus by individual GABAergic interneurons. *Nature* 1995; **378**: 75–78.
41 Kopell N, Ermentrout GB, Whittington MA, Traub RD. Gamma rhythms and beta rhythms have different synchronization properties. *Proc Natl Acad Sci USA* 2000; **97**: 1867–1872.
42 Buzsaki G, Wang XJ. Mechanisms of gamma oscillations. *Annu Rev Neurosci* 2012; **35**: 203–225.
43 Hyman JM, Hasselmo ME, Seamans JK. What is the functional relevance of prefrontal cortex entrainment to hippocampal theta rhythms. *Front Neurosci* 2011; **5**: 24.
44 Cobb SR, Buhl EH, Halasy K, Paulsen O, Somogyi P. Synchronization of neuronal activity in hippocampus by individual GABAergic interneurons. *Nature* 1995; **378**: 75–78.
45 Cunningham MO, Hunt J, Middleton S, LeBeau FE, Gillies MJ, Davies CH *et al.* Region-specific reduction in entorhinal gamma oscillations and parvalbumin-immunoreactive neurons in animal models of psychiatric illness. *J Neurosci* 2006; **26**: 2767–2776.
46 Lodge DJ, Behrens MM, Grace AA. A loss of parvalbumin-containing interneurons is associated with diminished oscillatory activity in an animal model of schizophrenia. *J Neurosci* 2009; **29**: 2344–2354.
47 Wulff P, Ponomarenko AA, Bartos M, Korotkova TM, Fuchs EC, Bahner F *et al.* Hippocampal theta rhythm and its coupling with gamma oscillations require fast inhibition onto parvalbumin-positive interneurons. *Proc Natl Acad Sci USA* 2009; **106**: 3561–3566.
48 Reynolds GP, Czudek C, Andrews HB. Deficit and hemispheric asymmetry of GABA uptake sites in the hippocampus in schizophrenia. *Biol Psychiatry* 1990; **27**: 1038–1044.
49 Meyer U, Nyffeler M, Yee BK, Kneusel I, Feldon J. Adult brain and behavioral pathological markers of prenatal immune challenge during early/middle and late fetal development in mice. *Brain Behav Immun* 2008; **22**: 469–486.
50 Belforte JE, Zsiros V, Sklar ER, Jiang Z, Yu G, Li Y *et al.* Postnatal NMDA receptor ablation in corticolimbic interneurons confers schizophrenia-like phenotypes. *Nat Neurosci* 2010; **13**: 76–83.
51 Richetto J, Calabrese F, Meyer U, Riva MA. Prenatal versus postnatal maternal factors in the development of infection-induced working memory impairments in mice. *Brain Behav Immun* 2013; **33**: 190–200.
52 Benson DL, Isackson PJ, Hendry SH, Jones EG. Expression of glutamic acid decarboxylase mRNA in normal and monocularly depreived cat visual cortex. *Mol Brain Res* 1989; **5**: 279–287.
53 Moser MB, Moser EI, Forrest E, Andersen P, Morris RG. Spatial learning with a minislab in the dorsal hippocampus. *Proc Natl Acad Sci USA* 1995; **92**: 9697–9701.
54 Fanselow MS, Dong HW. Are the dorsal and ventral hippocampus functionally distinct structures. *Neuron* 2010; **65**: 7–19.
55 Moser MB, Moser EI, Forrest E, Andersen P, Morris RG. Spatial learning with a minislab in the dorsal hippocampus. *Proc Natl Acad Sci USA* 1995; **92**: 9697–9701.

56 Ledoux AA, Boyer P, Phillips JL, Labelle A, Smith A, Bohbot VD. Structural hippocampal anomalies in a schizophrenia population correlate with navigation performance on a wayfinding task. *Front Behav Neurosci* 2014; **8**: 88.
57 Benetti S, Mechelli A, Picchioni M, Broome M, Williams S, McGuire P. Functional integration between the posterior hippocampus and prefrontal cortex is impaired in both first episode schizophrenia and the at risk mental state. *Brain* 2009; **132**: 2426–2436.
58 Narr KL, Thompson PM, Sharma T, Moussai J, Blanton R, Anvar B *et al.* Three-dimensional mapping of temporo-limbic regions and the lateral ventricles in schizophrenia: gender effects. *Biol Psychiatry* 2001; **50**: 84–97.
59 Oertel-Knochel V, Linden DE. Cerebral asymmetry in schizophrenia. *Neuroscientist* 2011; **5**: 456–467.
60 Hasen A, Schneider M, Schneider-Axmann T, Ruge D, Retz W, Rosler M *et al.* A similar but distinctive pattern of impaired cortical excitability in first-episode schizophrenia and ADHD. *Neuropsychobiology* 2013; **67**: 74–83.